ORIGINAL ARTICLE

Understanding the vulnerability of surface–groundwater interactions to climate change: insights from a Bavarian Forest headwater catchment

Muhammad Usman Munir[1] · Katharina Blaurock[1] · Sven Frei[2]

Abstract

Headwaters play a crucial role in maintaining forest biodiversity by providing unique habitats and are important for the regulation of water temperature and oxygen levels for downstream river networks. Approximately 90% of the total length of streams globally originate from headwaters and these systems are discussed to be especially vulnerable to impacts of climate change. This study uses an integrated hydrological model (HydroGeoSphere) in combination with 23 downscaled ensemble members from representative concentration pathways (RCPs) 2.6, 4.5 and 8.5 to examine how climate change affects water availability in a headwater catchment under baseflow conditions. The simulations consistently predict increasing water deficits in summer and autumn for both the near (2021–2050) and far future (2071–2099). Annual mean water deficits were estimated to be 4 to 7 times higher than historical levels. This is mainly due to a projected reduction in precipitation inputs of up to -22%, while AET rates remain similar to those observed during the historical reference period (1992–2018). The declining groundwater storage reserves within the catchment are expected to result in a significant decline in surface water availability during summer and autumn, with a reduction in mean annual stream discharge by up to 34% compared to the reference period. Due to declining groundwater levels, upstream reaches are predicted to become intermittent in summer leading to a reduction of the total stream flow length by up to 200 m. Findings from this study will enhance our understanding of future water availability in headwater systems and may aid in the development of effective management strategies for mitigating local impacts of climate change and preserving these vulnerable ecosystems.

Keywords Water availability in headwater catchment · Stream-aquifer interaction · Regional climate model · Integrated hydrological modelling

Introduction

Stream-aquifer interactions are characterized by dynamic exchange of water and solutes between the surface and subsurface flow domains. Direction and rate of water exchange controls instream biogeochemical conditions, hyporheic turnover of nutrients, moisture availability in riparian areas as well as temperature and water availability in riverine systems (Fleckenstein et al. 2006; O'Connor and Harvey 2008; Niswonger and Fogg 2008; Frei et al. 2009; Taie Semiromi and Koch 2020). Traditionally, three different types are used in literature to describe the nature of stream-aquifer interactions: (1) a gaining reach receives water from the aquifer when the instream hydraulic head is lower than that of the adjacent groundwater, (2) a losing reach occurs when the stream loses water to the aquifer due to a higher instream hydraulic head compared to the adjacent groundwater, and

✉ Muhammad Usman Munir
  muhammad.munir@uni-bayreuth.de

  Katharina Blaurock
  katharina.blaurock@uni-bayreuth.de

  Sven Frei
  sven.frei@wur.nl

1 Department of Hydrology, University Bayreuth,
   Universitätsstraße 30, 95447 Bayreuth, Germany

2 Department of Aquatic Ecology and Water Quality
   Management, Wageningen University and Research,
   Wageningen, Netherlands

(3) a disconnected stream describes the situation where there is no water-saturated connection to the groundwater facilitating high loss rates of stream water to the aquifer. The exchange of water between stream and groundwater can be highly variable in time and space due to the temporal dynamics of river flows and the geologic heterogeneity at the stream-aquifer interface (Conant 2004; Fleckenstein et al. 2006; Krause et al. 2007; Nyquist et al. 2008; Frei et al. 2009). Because of this high variability, it is often not possible to classify streams as purely gaining or losing (Baldwin and Mcguinness 1963). A stream reach, however, can be considered as net-gaining if it receives more water from the aquifer than it loses, and net-losing if the opposite is true.

When precipitation inputs are low, inflowing groundwater is often the only source that sustains streamflow under baseflow conditions (Delleur 1999). During droughts perennial streams maintain continuous surface flow because of groundwater inflow (Misra et al. 2011). Surface water availability during baseflow conditions is essential for preserving aquatic habitats and influencing water quality in rivers and streams (Beatty et al. 2010; Choi et al. 2018). A study conducted in Sweden during winter baseflow conditions showed the importance of groundwater, where inflows scaled non-linearly related to catchment size, ranging from approximately 20% for smaller headwater catchments to 80% for larger sized catchments (Peralta-Tapia et al. 2015). Similarly, Kaule and Gilfedder (2021) highlighted the significance of groundwater inflow for headwater catchments in Germany, where the fraction of instream groundwater increased from 10% under normal flow conditions to 70% during baseflow conditions in late summer. For the Upper Colorado River Basin, Miller et al. (2016) found that on average, 56% of river stream water originates from groundwater inflow. The balance between moderate flow conditions, floods, and droughts is crucial for the health of fluvial ecosystems (Richter et al. 1997; Arthington et al. 2006), and dropping groundwater levels can negatively impact ecological processes and biodiversity for these sensitive ecosystems (Choi et al. 2018).

According to IPCC (2014) there is an increase in global temperature and various aquatic ecosystems are at risk of serious impacts due to increasing water temperature and lower water availability. The projections for climate change indicate a significant reduction in the availability of groundwater by the end of the twenty-first century, leading to significant effects on both global and regional water resources (Atawneh et al. 2021; Wunsch et al. 2022). Recent studies for Central Europe found that climate change is expected to increase the duration and frequency of low flow conditions (Gosling et al. 2017; Marx et al. 2018) with an increase of evapotranspiration rates during summer until 2100 (Chan et al. 2021; Kaule and Frei 2022). For large areas in Germany it is predicted that climate change will increase the

probability of drought conditions due to higher evapotranspiration rates in summer that causes up to 43% annual reduction in the streamflow by 2050 (Huang et al. 2010; Al-Mukhtar et al. 2014). Goderniaux et al. (2009) and Wunsch et al. (2022) found that due to increased evapotranspiration and reduced percolation rates, groundwater storage is also likely to decline as a result of climate change. According to Natkhin et al. (2012) Northeast Germany has already seen a significant reduction in groundwater recharge between 1957 and 2007, primarily as a result of decreased precipitation and increased evapotranspiration rates.

Approximately 90% of the total length of streams globally originate from headwaters (Downing et al. 2012; Allen et al. 2018), making them crucial for downstream water availability and quality (Alexander et al. 2007). Headwater streams in general are often more dependent on groundwater inputs compared to downstream rivers and streams (Kaule and Gilfedder 2021). Because of the strong dependency of groundwater inputs and limited groundwater storage reserves, streamflow in headwater catchments is highly sensitive to climate change (Bennett et al. 2012). A shift in precipitation patterns, increasing temperature and less rainfall during dry seasons in summer significantly can impact the water availability in these systems with the potential to also disrupt the connection between headwater catchment and downstream river networks. Bernsteinová et al. (2015) observed that headwater catchments in Central Europe were already experiencing negative flow trends in summer due to an increase in temperature from 1978 to 2011. Kaule and Frei (2022) demonstrated that the water balance of headwater catchments located in the lower mountain ranges of Germany has been and will continue to be significantly affected by climate change, resulting in an increased frequency and intensity of drought events.

Quantification of interactions between surface water bodies (e.g., rivers and streams or lakes) and groundwater on different spatial and temporal scales can be estimated using integrated hydrological modeling frameworks (Frei et al. 2009; Chen et al. 2016). These modelling frameworks offer a comprehensive and integrated view of the hydrological cycle, accounting for interactions and feedbacks between surface and subsurface flow processes. By accounting for the complex dynamics and feedbacks between surface and subsurface water flow, integrated hydrological models enable a more accurate representation of hydrological systems and provide valuable insights into the impacts of human activities and climate change on the water cycle. Surface–groundwater interactions on various scales were intensively studied in the past using integrated hydrological models (e.g., Ala-aho et al. 2017; Chen et al. 2016; Cloutier et al. 2014; Frei et al. 2009; Min et al. 2015) but only a few studies focused on how these interactions are affected by climate change (Goderniaux et al. 2015; Molano-Leno et al. 2018).

As part of this study, our objective is to assess the influence of regional climate change on the water availability in a small headwater catchment located in the Bavarian Forest region of South-East Germany. This catchment can be seen as a representative system for many forested catchments located in the lower mountain ranges of Germany and Central Europe. For this purpose, we used the integrated hydrological model HydroGeoSphere (HGS) to represent hydrological processes in the catchment, including surface and subsurface flow as well as interactions between both flow domains. We utilized Regional Climate Models (RCMs) to predict future precipitation inputs, temperature, and potential evapotranspiration rates. These parameters were integrated into the HGS model to simulate runoff generation processes in the catchment. Specifically, we focused on examining the effects of climate change on instream water availability and exchange of water between the stream and groundwater during baseflow conditions in late summer. We hypothesize that climate change will result in a decrease in groundwater contributions to the stream, particularly during low flow conditions in summer, due to dropping groundwater levels. This hypothesis is based on the expectation that RCMs, with their predicted changes in precipitation, temperature, and actual evapotranspiration rates, will alter the hydrological cycle and decrease the availability of groundwater for streamflow. Results from this study will provide a better understanding on future water availability in headwater systems and might

help to develop efficient management strategies to mitigate local effects of climate change and to protect these sensitive ecosystems.

Methods

Study area

The Grosse Ohe catchment is situated in the Bavarian Forest National Park in South-East Germany (Fig. 1). It is the headwater catchment of the Grosse Ohe river, the largest tributary of the river Ilz which joins the Danube river at Passau, Germany. The catchment covers 19.2 km^2 area (mean terrain slope is 7.7°) and shares its border with the Czech Republic. Hinterer Schachtenbach having 3.5 km^2 area is the sub-catchment located in the Grosse Ohe catchment. The elevation of the Grosse Ohe catchment stretches from 770 to 1453 m.a.s.l. with a permanent lake (Rachelsee) located at an elevation of 1070 m.a.s.l. in the north of the catchment. The bedrock geology is characterized by two major rock types; biotite granite and cordierite-sillimanite gneiss. The main proportion of the soil consists of cambisol, while lithosol and histosol soil types also can be found in this catchment. Most of the area is covered with natural forest in which Norway Spruce is the dominant species (almost 70%) (Beudert et al. 2015). Annual rainfall in the Grosse Ohe catchment varies from 1350 to 1600 mm
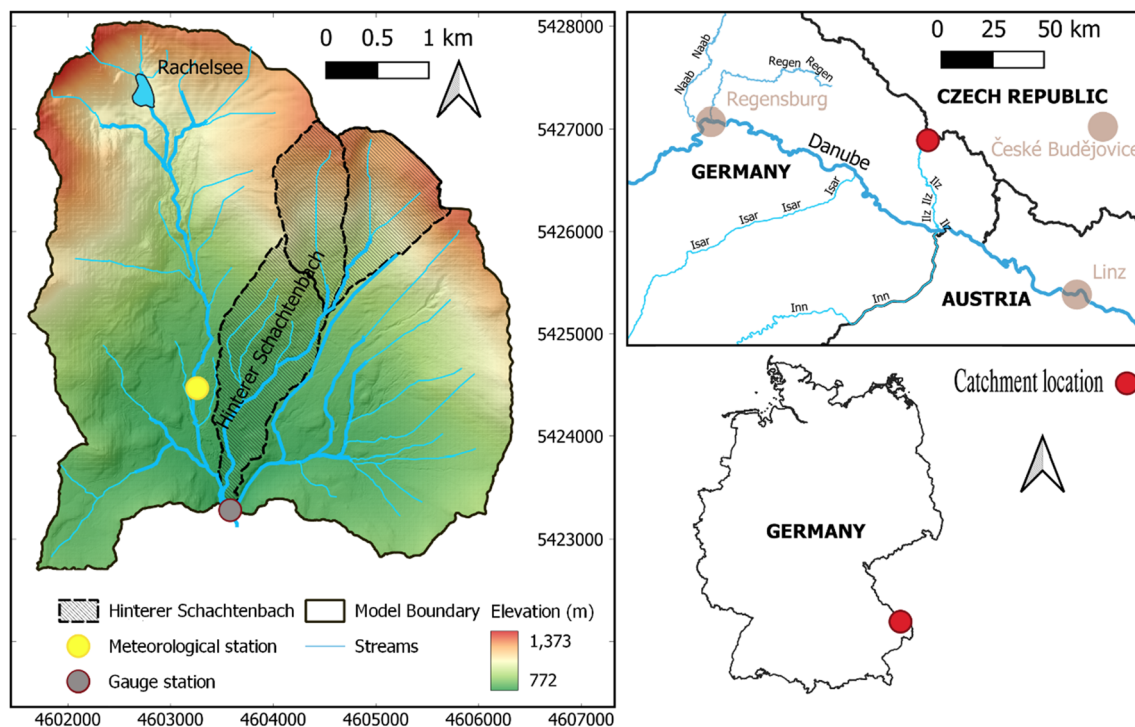
Fig. 1 Topographical map and location of the Grosse Ohe catchment and its sub-catchment Hinterer Schachtenbach, along with the downstream river network

yr^{-1} with a mean annual discharge of 2.663 mm/d measured at the Taferlruck gauging station located at the catchments' outlet (Fig. 1). Based on the climate, the catchment lies in the temperate zone and is affected by Atlantic and continental influences (Bässler 2008).

Hydrological modelling

HydroGeoSphere (HGS) is an integrated fully distributed, physical-based hydrological model that simultaneously represents surface and subsurface flow processes as well as interactions between the two flow domains (Therrien et al. 2008). A detailed model description along with all governing equations are available in detail in Aquanty Inc, (2015). In HGS, a control-volume finite element scheme is used to solve the governing equations for 3D variably saturated subsurface flow and 2D-depth averaged surface flow. HGS uses the diffusive wave approximation of the Saint–Venant equation for representing 2D-depth averaged surface flow, given as:

$$\frac{\partial \phi_o h_o}{\partial t} - \frac{\partial}{\partial x}\left(d_o K_{ox}\frac{\partial h_o}{\partial x}\right) - \frac{\partial}{\partial y}\left(d_o K_{oy}\frac{\partial h_o}{\partial y}\right) + d_o\Gamma_o \pm Q_o = 0 \tag{1}$$

In Eq. (1) ϕ_o [–] is the surface flow domain porosity, h_o [L] the surface water elevation, d_o [L] is surface water depth, K_{ox} and K_{oy} are surface conductances [L T^{-1}], Q_o [L T^{-1}] is a volumetric flow rate per unit area representing external source and sinks and Γ_o [L T^{-1}] represents fluid exchanges with the subsurface domain. Variably saturated subsurface flow is represented using the modified form of the 3D Richards' equation, given as:

$$-\nabla.(q) + \sum \Gamma_o \pm Q_{BC} = S_\omega S_s\frac{\partial \psi}{\partial t} + \theta_s\frac{\partial S_\omega}{\partial t} \tag{2}$$

where q [L T^{-1}] is the Darcy flux, Γ_o[L^3 L^{-3} T^{-1}] is symbolizes the exchange between surface and sub-surface domain, Q_{BC} [L^3 L^{-3} T^{-1}] is a volumetric flux that is associate with a boundary condition. ψ [L] is the hydraulic head, θ_s [–] is the porosity, S_ω and S_s [–] are the saturation and the specific storage coefficient, respectively. Surface and subsurface domains are linked using the dual node approach:

$$d_o\Gamma_o = \omega_m\frac{k_r K_{zz}}{l_{exch}}(h - h_o) + \omega_d\frac{k_{dr}K_{dzz}}{l_{exch}}(h_d - h_o) \tag{3}$$

where, h_o [L] is the surface water head, h and h_d [L] are the subsurface porous media and dual media hydraulic head respectively, k_r and k_{dr} [–] are the relative permeabilities, ω_d [–] is the volumetric fraction of the dual medium, K_{zz} and K_{dzz} [LT^{-1}] are the vertical saturated hydraulic conductivities l_{exch} [L] is a coupling length.

Daily potential evapotranspiration rates were calculated with the FAO Penman–Monteith equation (Allen et al. 1998)

based on the climatic available data (e.g. temperature, wind speed, relative humidity, solar radiation). HGS is calculating actual evapotranspiration based on the potential evapotranspiration rates using the method suggested by Kristensen and Jensen (1975). Here actual evapotranspiration is divided into three parts; evaporation from the canopy, transpiration from plants and evaporation from the soil. Root uptake of water (Tr) [LT^{-1}] is calculated using the relationship shown in Eq. (4).

$$Tr = f_1(LAI)f_2(\theta)RDF(E_p - E_{can}) \tag{4a}$$

$$f_1(LAI) = C_2 + C_1 LAI \tag{4b}$$

$$f_2(\theta) = 1 - \frac{(\theta_{FC} - \theta)^{C_3}}{(\theta_{FC} - \theta_{\omega p})} \tag{4c}$$

Here f_1(LAI) [–] is a function of the Leaf Area Index provided seasonally for each type of vegetation, C_1[–], and C_2[–], and $f_2(\theta)$[–] is a function of the soil moisture content, Root Distribution Function (RDF) defines the distribution of the roots with depth [-], E_p [LT^{-1}] is the potential evapotranspiration. C_3 [–] is a fitting parameter, $\theta_{\omega p}$ [–] is the moisture content at wilting point, θ_{FC} [-] is the moisture content at field capacity. Finally actual evaporation rates along with transpiration from soil surface and subsurface soil layers is estimated by Eq. 5

$$E_s = \alpha(E_p - E_{can})(1 - f_1(LAI)EDF) \tag{5}$$

where, α [–] is a wetness factor, E_{can} [LT^{-1}] is the canopy evaporation and EDF [–] is the evaporation density function and is assumed to be effective from soil surface to a given extinction depth.

Model setup, parametrization and boundary conditions

To achieve the objective of this study, we employed a nested modelling approach using HGS. This involved developing an HGS model for the entire Grosse Ohe catchment, as well as a separate model for one of its sub-catchments, Hinterer Schachtenbach (Fig. 2). As long-term discharge data were only available for the entire Grosse Ohe catchment, the larger model was used for calibration and validation, while the model for the sub-catchment, was used for investigating the impact of climate change on surface/groundwater interactions. Despite maintaining an accurate representation of surface/groundwater interactions, the sub-catchment model demonstrated greater computational efficiency than the larger catchment model. Due to its significantly lower runtimes, we utilized the sub-catchment model to simulate various long-term climate change scenarios.
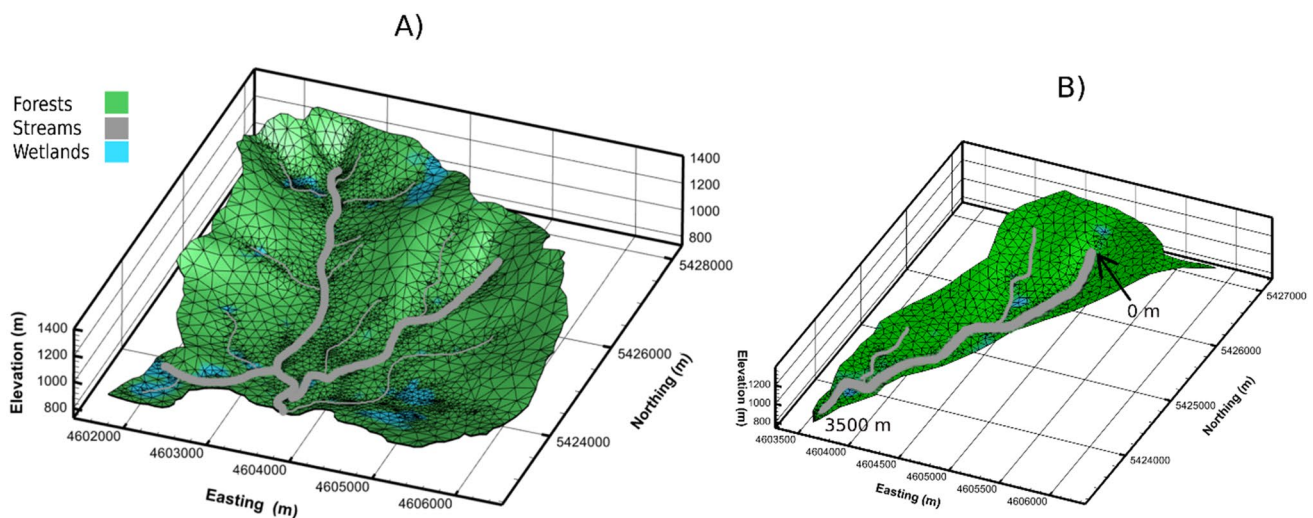
Fig. 2 Model discretization of the **A** Grosse Ohe catchment and **B** the sub-catchment Hinterer Schachtenbach. The label 0 and 3500 m refer to the total stream length used in Figs. 6 and 7

The computational grid for the surface flow domains of both models was generated using the preprocessor software AlgoMesh (HydroAlgorithmics Pty Ltd 2016). AlgoMesh calculates an optimal triangular finite element mesh based on the Delaunay criteria. To accurately represent surface/groundwater interactions, both models utilized a refined surface mesh in areas where these interactions were anticipated, such as stream locations and wetland areas (Fig. 2). The elevation of the surface nodes was obtained from a 5 m resolution digital elevation model (DEM). The final 2D mesh of the larger catchment model contains 3399 nodes and 6570 triangular elements, whereas the sub-catchment model includes 1824 nodes and 3507 triangular elements. To generate a 3D mesh for the subsurface flow domain, the 2D surface mesh was extended vertically by three main layers: a top layer with a thickness of 5 m, and middle and bottom layers with a thickness of 10 m each. Furthermore, the top layer was subdivided into multiple sub-layers, each with a thickness of 0.5 m. The vertical discretization was kept identical for both models to ensure consistency. The final 3D grid for the Grosse Ohe catchment comprises 40,788 nodes and 78,840 elements, while the sub-catchment grid consists of 21,888 nodes and 42,084 elements. Vertical discretization was implemented to represent the geological conditions within the two catchments with a shallow soil layer, a regolith main aquifer and an impermeable bedrock layer. Around 5.6% of the total area of the catchment are riparian wetlands with an average thickness of 1 to 2 m. Wetlands were represented using an exponentially decaying hydraulic conductivity (Ksat) distribution with depth, following the approach proposed by Frei et al. (2010). All Ksat values (wetlands, soil layer and regolith aquifer) were parameterized during the calibration process, and the final

values can be found in Table S1 as part of the supplement. Different overland flow and evapotranspiration properties were assigned to the forested and wetland areas as well as to the stream segments (see Table S1 supplement).

All boundary nodes at the catchment/sub-catchment boundaries in the surface and subsurface flow domains, except for the outlet nodes (surface flow domain), were set as no-flow boundaries. Additionally, the subsurface nodes representing the impermeable bedrock also were assigned as no-flow boundary conditions. A critical depth boundary was assigned to the surface nodes representing the outlet of the catchment/sub-catchment, allowing the water to leave the surface flow domain at the outlet location. Spatially uniform daily rainfall and evapotranspiration rates were applied as upper flux boundaries for both models to the surface flow domain. Precipitation is the combined input of rainfall and snowmelt. To simulate snowmelt, we utilized the HBV light model (Seibert 1997), which has been previously used in combination with process-based hydrological modeling, as presented in Kaule and Frei (2022). HBV uses the degree-day method to estimate snowmelt based on the air temperature.

Climate projections

The Intergovernmental Panel on Climate Change (IPCC) introduced the Representative Concentration Pathways (RCPs) in its fifth assessment report (AR5). These pathways play a crucial role in understanding the exploration of climate change simulations and long-term predictions up to 2100. The Regional Climate Model (RCM) output from the EURO-CORDEX and ReKlies project was used in this model and was provided and downscaled by the Bavarian

State Office for Environment (LFU). RCM is a time series of high-resolution climate data (0.11° or 12 km) for the period of 1951–2006 and future scenarios ranging from 2006 to 2100. The selection of GCM and downscaling is very important as every GCM has its strengths and shortcomings (IPCC 2014). The original RCM resolution is 12.5×12.5 km, but the LFU increased it to a 5×5 km grid resolution. The downscaling was carried out using the method proposed by Marke (2008). The presence of deviations between climate models and historical data is known as bias. This bias can be corrected using bias adjustment or bias correction methods. The bias adjustment method uses the Quantile Delta Mapping method (Cannon et al. 2015) and is widely used in various studies to adjust the bias between projected and observed data (Maraun 2013; Rajczak et al. 2016; Kim et al. 2016; Ngai et al. 2017; Ringard et al. 2017; Reiter et al. 2018). In order to evaluate potential impacts of climate change on stream water availability for the sub-catchment, in total we used 23 downscaled projections as input to the HGS model (6 from RCP 4.5, 8 from RCP2.6 and 9 from RCP 8.5, Table 1), detailed RCMs with their names are provided in Table 1. Each projection was split into two periods: (1) near future 2021–2050 and (2) far future 2071–2099. As

a reference we additionally simulated the period from 1992 to 2018 based on available historical data. To investigate the impact of climate change on water balance components, each projection was simulated separately. Notably, each ensemble member contributed equally to the ensemble mean with a uniform weighting. The ensemble means of precipitation, evapotranspiration, discharge, and storage change for each pathway were calculated and compared with the reference period.

Results

Model performance

The model was calibrated for the water year 2017 (11/01/2017–10/31/2018) based on available daily runoff data measured at the outlet of the Grosse Ohe catchment. Due to the high computational demand of the large catchment model and associated long simulation runtimes, calibration was performed manually. Using only a single hydrological year for model calibration is frequently employed when utilizing process-based and fully distributed

Table 1 Overview of the average annual temperature and total annual precipitation for the applied climate change scenarios

GCM	RCP	RCM	Institute	T [°C] 2021–2050	P [mm] 2021–2050	T [°C] 2071–2099	P [mm] 2071–2099
EC-EARTH	rcp2.6	CCLM4-8–17	CLMcom	8.24	1140.1	8.4	1169.1
EC-EARTH		RACMO22E	KNMI	8.47	1175.0	8.6	1197.3
EC-EARTH		RCA4	SMHI	8.67	1097.5	8.8	1114.1
MIROC		CCLM4-8–17	CLMcom	9.01	1000.0	9.1	1048.2
MPI		WETTREG2018	CEC	8.35	1101.3	8.4	1085.8
MPI		CCLM4-8–17	CLMcom	8.33	1189.0	8.2	1155.8
MPI		RCA4	SMHI	8.87	1171.7	8.7	1100.5
MPI		WRF361H	UHOH	8.53	1088.2	8.6	1009.8
EC-EARTH	rcp4.5	CCLM4-8–17	CLMcom	8.45	1100.0	9.3	1182.1
EC-EARTH		RACMO22E r12	KNMI	8.75	1190.5	9.8	1228.9
EC-EARTH		RCA4	SMHI	8.85	1125.6	10.0	1193.0
EC-EARTH		RACMO22E	KNMI	8.86	1105.1	9.8	1120.7
MPI		CCLM4-8–17	CLMcom	8.22	1184.3	8.9	1173.8
MPI		RCA4	SMHI	8.67	1155.8	9.6	1185.7
EC-EARTH	rcp8.5	CCLM4-8–17	CLMcom	8.71	1176.5	11.0	1132.4
EC-EARTH		RACMO22Er12	KNMI	9.06	1234.4	11.6	1246.9
EC-EARTH		RCA4	SMHI	9.24	1176.4	12.0	1163.4
EC-EARTH		RACMO22E	KNMI	8.97	1147.4	11.5	1220.6
EC-EARTH		WRF361H	UHOH	8.84	1139.5	11.2	1044.5
MPI		WETTREG	CEC	8.78	1059.8	11.0	992.3
MPI		CCLM4-8–17	CLMcom	8.31	1174.4	10.5	1219.4
MPI		RCA4	SMHI	8.69	1136.3	11.5	1268.5
MPI		WRF361H	UHOH	8.43	1078.0	10.7	1045.9

Each scenario corresponds to a combination of a Global Climate Model (GCM) and a Regional Climate Model (RCM)

hydrological models (e.g. Cornelissen et al. 2013; Glaser et al. 2016; De Schepper et al. 2017; Kaule and Frei 2022). Validation was performed for the water years 2004–2017 (11/01/2004–10/31/2017). Figure 3 presents the observed and simulated discharge of the Grosse Ohe catchment during the calibration and validation period. The Nash–Sutcliffe-Efficiency (NSE) for the calibration period was estimated at 0.61, suggesting a satisfactory agreement between the observed and simulated discharge values. Despite a slightly lower NSE value of 0.51 for the validation period, the performance of the process-based hydrological model remains acceptable (Moriasi et al. 2007). Especially during low flow conditions in summer/early autumn, discharge was represented very well by the HGS model, as suggested by the high NSE score of 0.67 for this period. The simulations, however, proved challenging when high flow conditions were encountered since peak discharges were often systematically underestimated. This discrepancy can be partly attributed by the underestimation of precipitation rates during snow-melting events in winter and spring, as predicted by the degree-day method. Additionally, the insufficient resolution of the DEM used in the study is unable to capture the small-scale topographical features (stream width < 1 m) of the stream network, contributing to the disparity between the observed and simulated discharge values during high flow events.

Impact of climate change on the water balance components

The water balance of a catchment is a representation of the balance between precipitation (P), actual evapotranspiration (AET), discharge (Q), and storage change (ΔS). These components can help in understanding the changing hydrological conditions. Table 2 shows the mean annual water balance components for the different RCP ensembles utilized in the sub-catchment model. Figure 4 illustrates the seasonally-averaged water balance components for the sub-catchment, for the water years 2021–2050 (A, C, E, G), 2071–2099 (B, D, F, H), with the reference period of 1992–2018. According to the near future simulations using ensembles from RCP 2.6, 4.5 and 8.5, the annual average precipitation (including both rainfall and snowmelt) is expected to decrease by – 9%, – 12%, and – 12%, respectively, compared to the reference period (Table 2). The far future simulations using ensembles from RCP 2.6, 4.5, and 8.5 suggest that the annual average precipitation inputs will decrease by -15%, -11%, and -22%, respectively, compared to the reference period (Table 2). Figure 4A, indicates that all simulated RCP ensembles demonstrated a similar trend for precipitation, with a substantial decrease in seasonally averaged precipitation rates during spring, summer, and autumn. For summer, the season where baseflow conditions are mostly relevant, ensemble simulations for RCP 8.5 for the far future showed the lowest seasonally averaged precipitation inputs with a decrease of 141 mm compared to the reference period (Fig. 4B). According to the simulations across all RCP ensembles, average winter precipitation (including rainfall and snowmelt) is projected to increase significantly. This increase can be attributed to a shift from snowfall towards rainfall and snowmelt, which is caused by higher predicted temperatures during winter.

In comparison to the reference period, the average annual rates of AET shown in Table 2 were similar for the near and far future simulations using RCP 2.6 (-4% and -3%) and RCP 4.5 (– 3% and – 0.5%). For the RCP 8.5 ensemble, average annual AET decreased by -4% for the near future and
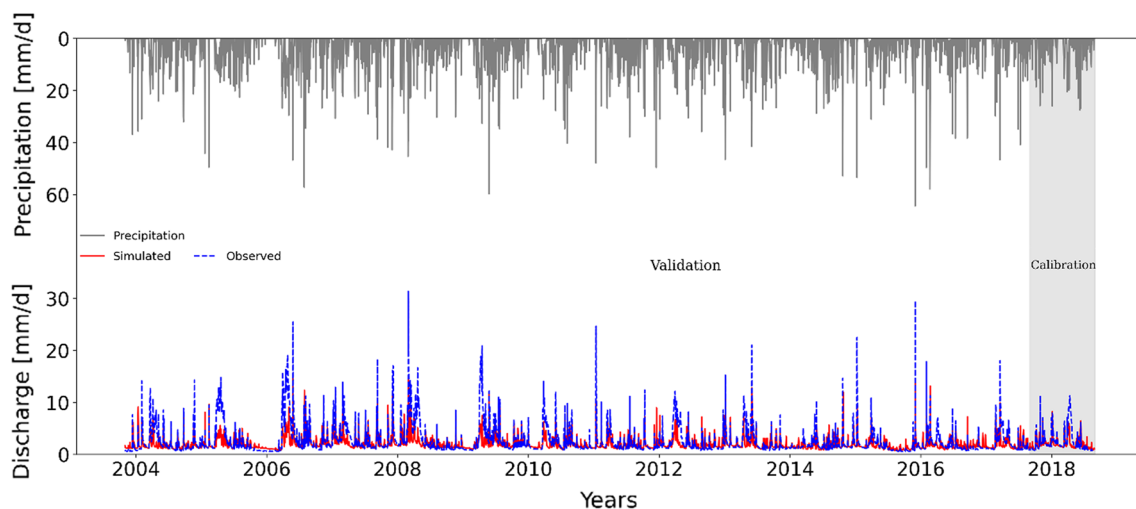
Fig. 3 Simulated and observed discharge for the calibration (11/01/2017–10/31/2018) and validation (11/01/2004–10/31/2017) period. NSE for the calibration period is 0.61 and for the validation period 0.51

Table 2 Average annual components of the water balance of the sub-catchment for the different RCP ensembles and the historical reference period

Parameters	Historic [mm/a]	Scenarios	RCP2.6 [mm/a]	RCP4.5 [mm/a]	RCP8.5 [mm/a]
Discharge	716	2021–2050	700 (~ − 2%)	694 (~ − 3%)	658 (~ − 8%)
		2071–2099	597 (~ − 17%)	657 (~ − 8%)	469 (~ − 34%)
Precipitation	1330	2021–2050	1210 (~ − 9%)	1171 (~ − 12%)	1175 (~ − 12%)
		2071–2099	1131 (~ − 15%)	1181 (~ − 11%)	1034 (− 22%)
AET	630	2021–2050	605 (~ − 4%)	608 (~ -3%)	603 (~ − 4%)
		2071–2099	610 (~ − 3%)	627 (~ − 0.5%)	675 (+ 7%)
Storage Change	− 16	2021–2050	− 95 (~ − 494%)	− 131 (~ − 719%)	− 86 (~ − 438%)
		2071–2099	− 76 (~ − 375%)	− 103 (~ − 544%)	− 110 (~ − 588%)

The percentage in parentheses represent the relative change of the components to the historical reference period. The scenarios include near future (2021–2050) and far future (2071–2099) simulations for RCP 2.6, RCP 4.5, and RCP 8.5

Q discharge, *AET* actual evapotranspiration, *P* precipitation

increased by + 7% for the far future simulations (Table 2). On a seasonal basis, the average AET rates for all RCP ensembles in the near future simulations were lower compared to the reference period, and this trend was observed across all seasons (Fig. 4E). In the far future simulations, particularly, simulations using the RCP 8.5 ensemble showed the highest seasonally averaged AET for all seasons (Fig. 4F). Simulations revealed a general reduction in surface water availability on an annual basis (Table 2), where average discharge decreased by − 2%, − 3%, and − 8% (for RCP 2.6, 4.5 and 8.5, respectively) in the near future, and a severe reduction by − 17%, − 8%, and − 34% (for RCP 2.6, 4.5 and 8.5, respectively) in the far future simulations. In the near future, simulations using all RCPs showed a notable increase in seasonally averaged discharge during winter when compared to the reference period. However, for spring, summer, and autumn, a decrease in discharge was observed across all RCP ensembles. Simulations for all RCPs suggested a significant decrease in seasonally averaged discharge for the far future. Lowest discharge values were simulated during baseflow conditions in summer and autumn, with a maximum decrease of up to − 50% for RCP 8.5 when compared to the reference period.

Table 2 shows that on average there was a slight water deficit of approximately − 16 mm per year during the reference period. However, it's important to note that although this value is negative, the past conditions in the catchment can be considered as neutral. This is because the long-term storage changes in the catchment were relatively stable and did not result in significant overall gains or losses of water. For the near and far future simulations, average annual storage change revealed a substantial increase in water deficits for all RCP ensembles ranging from − 375 to − 719% when compared to the reference period (Table 2). A seven-fold increase in water deficit was predicted using the RCP 4.5 ensemble for the near future and a six-fold increase was predicted using RCP 8.5 for the far future. Figure 4G and

H present the simulated values for the seasonally averaged storage change, wherein a positive value indicates that the catchment is gaining more water than it is losing, with water primarily stored in the subsurface (unsaturated zone + groundwater). Negative values correspond to situations where the catchment is losing more water than it is receiving, highlighting a deficit in the overall water budget. Based on the presented seasonally averaged storage change especially spring and summer is affected by increasing water deficits as was predicted by all RCP ensembles in the near and far future simulations. On average, simulations for all RCP ensembles predict an excess of water during winter and autumn, although average storage changes are only slightly positive during autumn. This trend of increasing water deficits becomes even more pronounced in the period 2071–2099, with a significant shift in the water balance towards negative values, particularly in spring and summer. Statistical significance in the differences between the historical and the climate change scenarios was assessed through a *t* test where $\alpha = 0.05$.

Impact of climate change on stream-aquifer interactions

For the sub-catchment simulations the total amount of groundwater inflow into the stream (exfiltration rates in Fig. 5) was estimated for all RCP simulations on a seasonal basis. In both near and far future simulations, seasonally averaged exfiltration rates show a significant decrease when compared to the historical reference period, indicating a severe reduction in groundwater availability for stream flow. Particularly during summer and autumn seasonally averaged exfiltration rates showed a substantial decrease by up to − 30% (RCP 8.5) compared to the reference period. Highest decreases in exfiltration rates throughout all seasons were simulated for the RCP 8.5 ensemble.

To better understand the potential consequences of declining groundwater levels in the sub-catchment under baseflow conditions, we investigated local surface-aquifer interactions by extracting spatially distributed exchange fluxes along the stream in the sub-catchment. Figure 6 presents the spatially distributed exchange fluxes extracted for all RCP ensembles and for all stream nodes in the sub-catchment model, ranging from spring areas ($X = 0$ m) down to the sub-catchment's outlet ($X = 3500$ m). Due to the unavailability of spatially distributed data across all RCP simulations and days during the summer and late autumn period, we made the choice to designate a reference day for the purpose of evaluating groundwater-surface water interactions. To determine an appropriate reference day, we conducted an analysis of historical data spanning from 2002 to 2018, as well as predicted discharge from various RCP scenarios. Our analysis consistently revealed that the lowest mean discharge consistently took place in late summer, specifically in September. Consequently, we settled on the 15th of September as our reference day. For each RCP ensemble member and the reference period, the 15th September of each year consequently was selected for which the local exchange fluxes were estimated.

Gaining stream sections are indicated by positive flux rates, while losing sections are indicated by negative rates. The flux rates for the reference period, which are presented as the average values estimated for the historic reference period (blue lines in Fig. 6), show that most stream sections in the past received water due to groundwater inflow. There are some stream reaches in the reference simulations where flux rates are negative indicating losing conditions. These losing conditions can be attributed to local topographical features (e.g. break in slope). In Fig. 6, the areas shaded in grey depict the range of variation for the extracted exchange fluxes observed among the different simulations belonging to a specific RCP ensemble. All RCP ensembles show a similar trend of decreasing exchange fluxes between stream and aquifer. While certain stream Sects. (1000 m > X > 1500 m) exhibit a notable resilience to water deficits during summer (with exchange fluxes only marginally different from those observed during the reference period), the majority of both the upstream and downstream sections show a significant reduction in groundwater inflow due to declining groundwater levels. Especially the stream reaches close to upstream spring areas ($X < 750$ m) were most affected by the water deficit in the different RCP ensembles e.g. where exchange rates drop by up to ~88% (RCP 8.5 far future) compared to the reference period and where entire stream sections turn from gaining into losing sections ($X < 250$ m). This trend can be observed among all RCP ensembles and for the near as well as far future simulations.

Figure 7 illustrates the effect of the declining trend in groundwater inflow on surface water availability during baseflow conditions in the sub-catchment. For the reference day (September 15th), the average surface water depths in the past (historical reference period) ranged from 2.5 cm in the upstream spring areas to approximately 0.5 m at the sub-catchments' outlet. Simulation results for the historical reference period indicate that there was always sufficient instream water available from baseflow to sustain a continuous streamflow for all sections of the stream within the sub-catchment. For the near future simulations (Fig. 7), all RCP ensembles predicted a significant decrease in surface water availability along the entire stream. Despite maintaining a continuous stream flow for the lower sections, the near-future simulations (Fig. 7A, C and E) show a significant decrease in surface water availability by up to 47% for the entire stream. However, due to falling groundwater levels and associated water loss to the aquifer, the most upstream sections ($X < 100$ m) in all RCP ensembles are projected to fall dry. A similar trend, with even less surface water availability (here water depths decrease by up to 50% compared to the reference period), is predicted for the far future (Fig. 7B, D and F).

Discussion

In this study we used an integrated hydrological model to investigate how local climate change affects the water availability of a headwater catchment under baseflow conditions. Particularly, we focused on three different aspects: the impact of climate change on (1) the different components of the annual/seasonal water balance, (2) interactions between the stream and aquifer, and (3) availability of surface water resources. Model calibration and validation results revealed a good overall model performance, with NSE values of 0.61 and 0.51, respectively. These values are consistent with those typically reported in studies utilizing catchment-scale hydrological models (e.g. Glaser et al. 2016; Kaule and Frei 2022; Partington et al. 2013). The model accurately represented catchment discharge under baseflow conditions. Simulations, however, proved challenging when high flow conditions were encountered since peak discharges were often systematically underestimated. This discrepancy can be partly attributed to the underestimation of snow-melting in winter and spring, as predicted by the degree-day method. Further, precipitation rates were spatially uniformly distributed over the catchment area, and the temporal model resolution required daily input data. Since intensive rainfall events can take place on temporal scales of minutes to hours, discharge peaks might have been missed in the model.

The study's predictions for the near and far future were generated using ensemble means derived from simulations of multiple ensemble members from different RCPs. Notably, each member contributed equally to the ensemble mean with uniform weighting. Ensemble members are usually
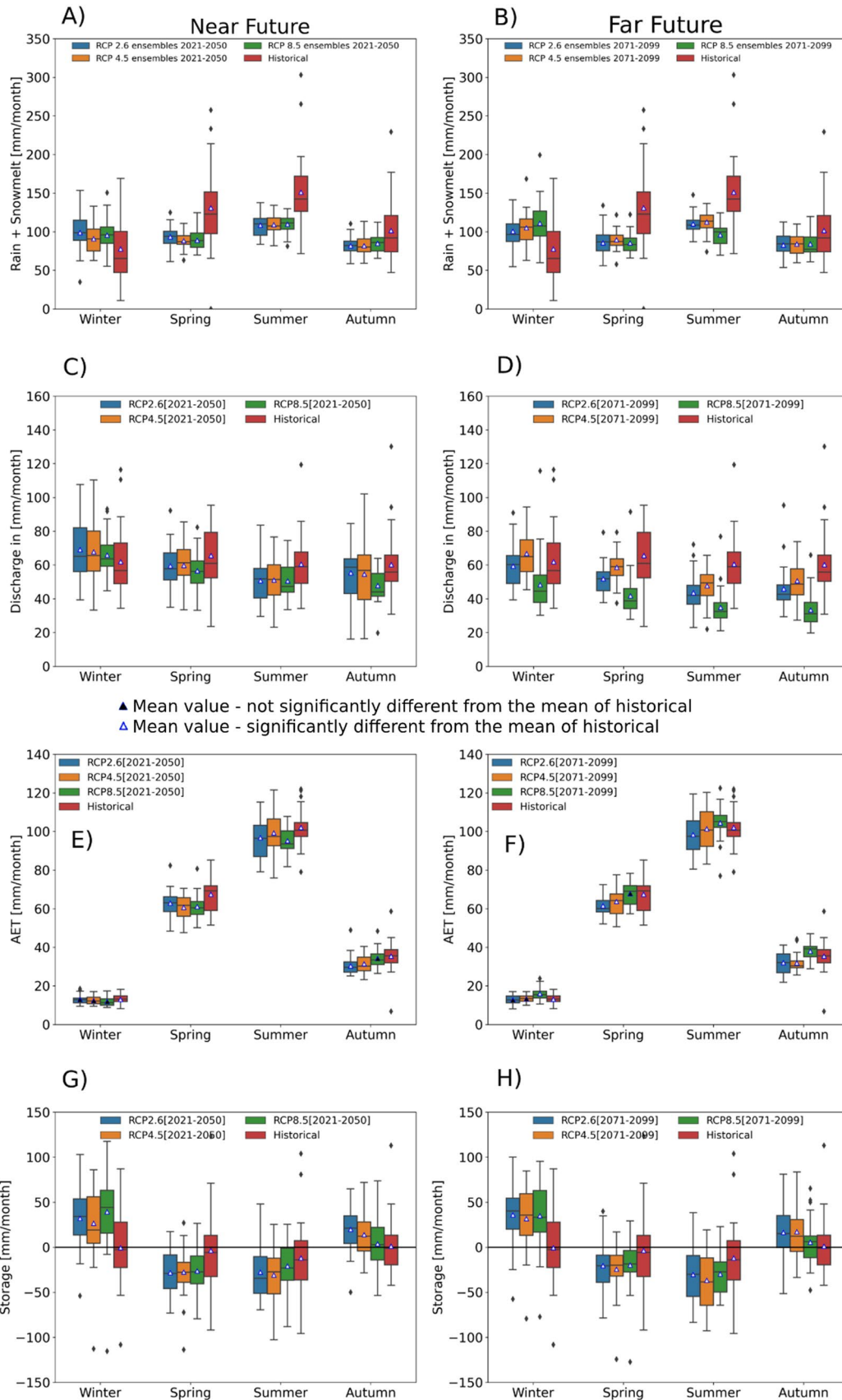
◀**Fig. 4** Mean water balance components for the Hinterer Schachtenbach sub-catchment, presented seasonally for both the near future (2021–2050) and far future (2071–2099), across all Representative Concentration Pathway (RCP) projections. **A**, **B** Seasonally-averaged monthly precipitation (P) (mm/month); **C**, **D** Seasonally-averaged monthly discharge (Q) (mm/month); **E**, **F** Seasonally-averaged monthly actual evapotranspiration (AET) (mm/month); **G**, **H** Seasonally-averaged monthly storage change (ΔS) (mm/month) The box represents the interquartile range (IQR), which spans from the 25th percentile (Q1) to the 75th percentile (Q3), with the median indicated by the line inside the box. The whiskers extend to the minimum and maximum values within 1.5 times the IQR from the upper and lower quartiles, respectively. Any data points outside of this range are displayed as points, representing potential outliers. Difference is significant at $\alpha = 0.05$

chosen randomly from a larger population, which can introduce statistical biases and raise concerns about their representativeness for the whole population. One way to compensate for this, is to employ as many ensemble simulations as possible (Kaule and Frei 2022). In our study we used all ensemble members that were available at the required resolution, which in total included 23 members from 3 different RCPs. Since the downscaling of the scenarios was performed by the Bavarian State Office for Environment (LFU) rather than by ourselves, we had to depend on the available number of ensemble members provided to us. Varying model performances of different ensemble members can introduce biases into the simulation results that might be compensated by using non-uniform weights. Weighting methods, however, require detailed information such as each member's skill, error, and noise, which is often unavailable (Weigel et al. 2010). Hence, Weigel et al. (2010) recommended equal weights as the safest of all possible methods.

Across all RCP simulations, there is a consistent change towards increasing water deficits in summer and autumn predicted for both near and far future scenarios. The simulations showed that the annual average water deficits were approximately 4 to 7 times higher than those observed during the historical reference period. Highest water deficits of ~ – 590% and ~ – 720% were simulated for RCP 4.5 (near future) and RCP 8.5 (far future), respectively. Increasing water deficits can be primarily attributed to the projected reduction in precipitation inputs by up to – 22%, as opposed to AET rates which remain similar to those observed during the historical reference period. Only the RCP 8.5 far future ensemble showed a significant increase of 7% in mean annual AET rates. These findings differ from results of other studies that predict a general decrease in precipitation inputs and a significant shift towards increasing AET rates for European headwater catchments (e.g. Benčoková et al. 2011; Kaule and Frei 2022). A limitation of our study is that potential shifts in the compositions and distribution of vegetation were not accounted for in our simulations. However, it is highly likely that the vegetation composition, particularly in

tree species, will undergo changes in the next 80–100 years. Reasons for this are adaptation to more frequent and longer drought conditions or infestation by pests such as bark beetles. Changes in plant communities are likely to affect AET rates and, consequently, will also impact water availability in the catchment. Incorporating vegetation changes into our simulations would require detailed scenarios regarding the timescales of transition as well as vegetation-specific parameters that can be used to estimate AET. However, developing scenarios for future vegetation composition is outside the scope of our expertise and beyond the objectives of our study.

Prolonged water deficit conditions resulted in declining groundwater storage reserves within the catchment. As a result of declining groundwater levels and the associated reduction in baseflow input, the stream network within the catchment is expected to undergo a significant decline in surface water availability especially during summer and autumn. A reduction in annual mean stream discharge by up to – 34% compared to the reference period was evident across all emission scenarios and is most notable during baseflow conditions in the late summer and early autumn months. The analysis of spatial exchange fluxes during the historical reference period indicated that the catchment's stream is primarily gaining water from groundwater inflow during baseflow conditions. There are some reaches in the simulations where the stream loses water to the aquifer, which can be explained by local topographical features such as breaks in slope. Small-scale transitions between gaining and losing conditions as a consequence of topography or instream obstacles such as beaver dams or dead trees has been described in literature as a common feature of headwater catchments (Huntington and Niswonger 2012; Majerova et al. 2015). The RCP simulations indicate that a reduction in absolute exchange rates will affect all stream reaches, including those with gaining and losing conditions, as well as those located in higher and lower areas of the catchment. However, for upstream reaches the reduction of groundwater inflow under baseflow conditions has severe consequences for the surface water availability as the stream becomes temporarily intermittent. Consequently, during summer and autumn it is predicted that the stream network within the catchment will diminish by up to 200 m, as upstream reaches near spring areas dry up as they lose the connection to the local groundwater. Similar findings were presented in Ward et al. (2020) that were examining stream network dynamics for headwater catchments in the U.S. Pacific Northwest. Here it was predicted that Oregon's headwaters could experience a 25% decrease in flow pathways during the driest months, ultimately leading to a reduction in the length of flowing river networks. Similarly, Kaule and Gilfedder, (2021) highlighted that in the lower mountain ranges of central Europe, extreme
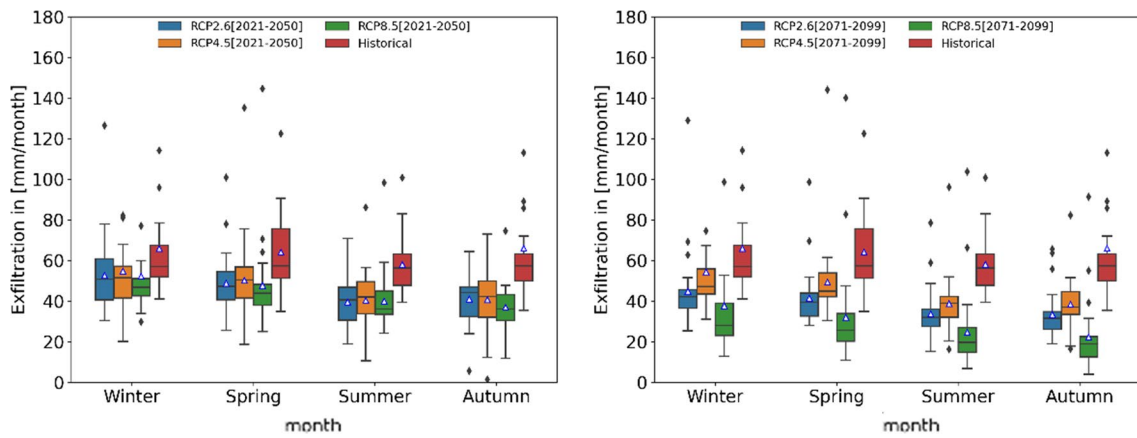
Fig. 5 Seasonally averaged total exfiltration rates between the groundwater and stream (exfiltration = inflow of groundwater to the stream) for the near and far future simulations and reference period


Fig. 6 Illustrates the projected flux exchange between the stream and aquifer in m/d during baseflow conditions in late summer. The flux rates were estimated for September 15th for all RCP ensembles and the reference period, and the blue line represents the mean exchange flux for the reference period (1992–2018). The grey shaded area indicates the range of variation in the exchange rates for the different RCP scenarios

weather events and prolonged drought conditions could potentially leading to stream disconnection and a severe reduction in surface water availability under climate change conditions.
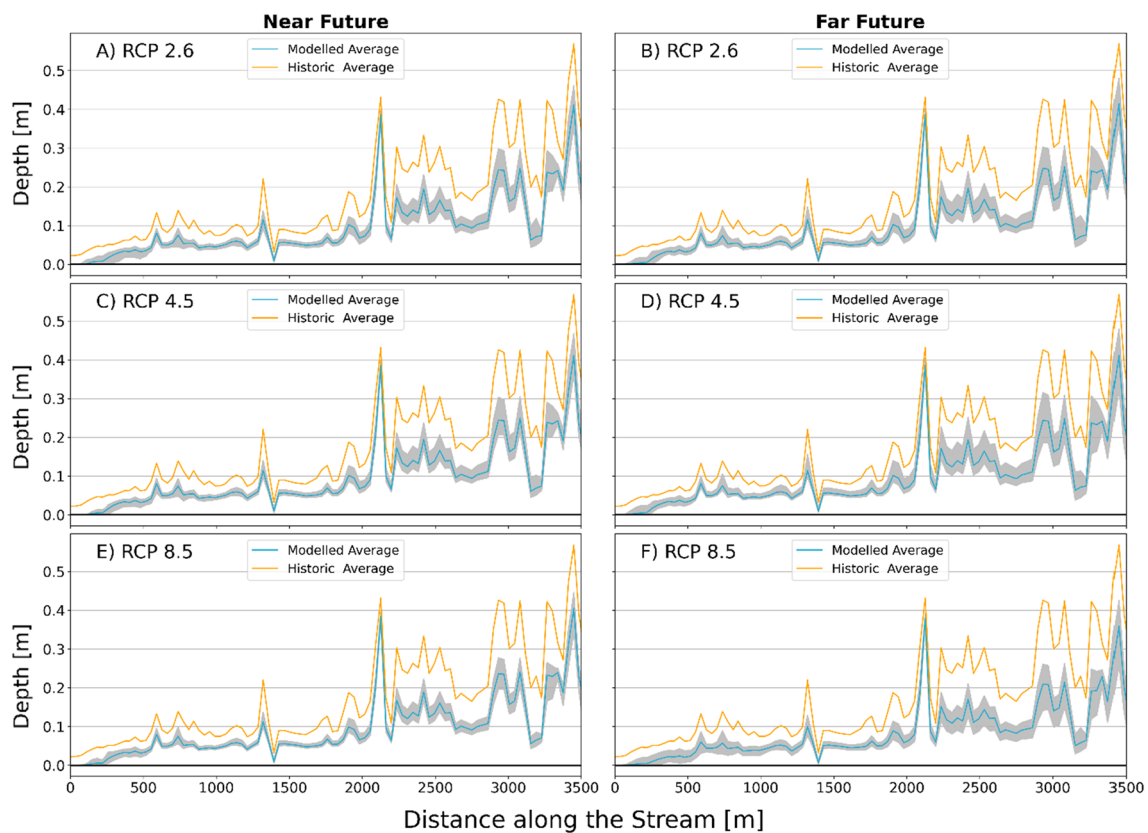
Fig. 7 Projected surface water depths for the stream during baseflow conditions in late summer. Water depths were estimated for September 15th for all RCP ensembles and the reference period, and the blue line represents the mean water depth for the reference period (1992–2018). The grey shaded area indicates the range of variation in water depths for the different RCP scenarios

Conclusions and implications

Our study aimed to investigate the impact of regional climate change on the water availability of a small headwater stream in the Bavarian Forest region of Germany. We used an integrated hydrological model in combination with multiple ensembles from different Representative Concentration Pathways (RCPs) to examine the potential effects of climate change on the stream's water resources. Simulations indicated:

(1) A significant decrease in precipitation inputs for the near (2021–2050) and far future (2071–2099).
(2) Rates of actual evapotranspiration that are comparable when related to the historical reference period (1992–2017).
(3) Prolonged water deficit conditions in future, resulting in declining groundwater levels in the catchment.
(4) A significant reduction in groundwater inflow during baseflow conditions leading to a temporal intermittence of the stream for upstream reaches
(5) A reduction of the total flow length by up to 200 m for the stream network in the catchment

These findings potentially can have significant implications for the ecosystem, as decreasing water availability may lead to changes in the water flow regime, increased water temperature and lower oxygen availability. Especially spring ecosystems depend on the continuous supply of groundwater and in mid mountain ranges are characterized by low temperature variability (Biggs et al. 2016). These ecosystems are recognized as biodiversity hotspots that serve as habitats for a diverse range of species that occupy various ecotonal niches (Cantonati et al. 2012). Supply of groundwater from spring areas is important for the regulation of water temperature and oxygen levels for downstream reaches, which is especially relevant during hot summer months when water temperatures can reach stressful levels for aquatic organisms (Power et al. 1999). Springs are the birthplace of 1st order streams, typically located in the upstream areas of headwater catchments. Our simulations have demonstrated that upstream reaches are especially vulnerable to the effects of decreasing groundwater levels, with a high likelihood that streams in these areas will become intermittent in summer (as was projected by all RCP scenarios). For spring areas this could mean that water supply from groundwater will

decrease substantially or could be interrupted entirely with fatal consequences for these sensitive ecosystem and the associated ecosystem services.

Headwaters play a crucial role in maintaining forest biodiversity by providing unique habitats, but they are also particularly vulnerable to the effects of climate change as was shown by our simulations and various other authors (e.g. Brooks 2009; Estrela-Segrelles et al. 2023; López-de Sancha et al. 2022; Ward et al. 2020). The anticipated increase in air temperatures, coupled with declining inputs from groundwater sources, is expected to cause a shift towards higher water temperatures in future (Van Vliet et al. 2013). For higher water temperatures, transmission rates of certain diseases can increase, posing health risks to freshwater species such as fish (Karvonen et al. 2010). All RCP scenarios predict a decline in summer precipitation, which, when combined with reduced groundwater supply and increasing water temperatures, may lead to lower dissolved oxygen concentrations and increased biological oxygen demand in headwater streams, thereby posing a threat to aquatic life (Whitehead et al. 2009). Plant communities that have adapted to high water saturation environments, such as riparian areas or wetlands, will be impacted by the decreasing availability of surface water during droughts, potentially resulting in a reduction in the size of these areas over time (Dwire et al. 2018). Once headwater streams become intermittent, species communities unadopted to such dry conditions might face trouble to regain vitality fast which might lead to a shift in the species composition (Majdi et al. 2020).

Supplementary Information The online version contains supplementary material available at https://doi.org/10.1007/s12665-023-11314-2.

Declarations

References

Ala-aho P, Soulsby C, Wang H, Tetzlaff D (2017) Integrated surface-subsurface model to investigate the role of groundwater in headwater catchment runoff generation: a minimalist approach to parameterisation. J Hydrol 547:664–677. https://doi.org/10.1016/J.JHYDROL.2017.02.023

Al Atawneh D, Cartwright N, Bertone E (2021) Climate change and its impact on the projected values of groundwater recharge: a review. J Hydrol 601:126602

Alexander RB, Boyer EW, Smith RA et al (2007) The role of headwater streams in downstream water quality1. JAWRA J Am Water Resour Assoc 43:41–59. https://doi.org/10.1111/J.1752-1688.2007.00005.X

Allen RG, Pereira LS, Raes D, Smith M (1998) Crop evapotranspiration —guidelines for computing crop water requirements. FAO Irrigation and drainage paper 56. Food and Agriculture Organization, Rome. p 290

Allen GH, Pavelsky TM, Barefoot EA et al (2018) Similarity of stream width distributions across headwater systems. Nat Commun 91(9):1–7. https://doi.org/10.1038/s41467-018-02991-w

Al-Mukhtar M, Dunger V, Merkel B (2014) Assessing the impacts of climate change on hydrology of the upper reach of the spree river: Germany. Water Resour Manag 28:2731–2749. https://doi.org/10.1007/s11269-014-0675-2

Aquanty (2015) HydroGeoSphere: a three-dimensional numerical model describing fully-integrated subsurface and surface flow and solute transport, Groundwater Simulations Group. Univ Waterloo

Arthington AH, Bunn SE, Poff NLR, Naiman RJ (2006) The challenge of providing environmental flow rules to sustain river ecosystems. Ecol Appl 16:1311–1318. https://doi.org/10.1890/1051-0761(2006)016[1311:TCOPEF]2.0.CO;2

Baldwin HL, Mcguinness CL (1963) A primer on ground water. U.S. Government Printing office, Washington, D.C.

Bässler C (2008) Climate change-trend of air temperature in the Innerer Bayerischer Wald (Bohemian Forest). Silva Gabretta 14:1–18

Beatty SJ, Morgan DL, McAleer FJ, Ramsay AR (2010) Groundwater contribution to baseflow maintains habitat connectivity for *Tandanus bostocki* (Teleostei: Plotosidae) in a south-western Australian river. Ecol Freshw Fish 19:595–608. https://doi.org/10.1111/j.1600-0633.2010.00440.x

Benčoková A, Krám P, Hruška J (2011) Future climate and changes in flow patterns in Czech headwater catchments. Clim Res 49:1–15. https://doi.org/10.3354/CR01011

Bennett KE, Werner AT, Schnorbus M (2012) Uncertainties in hydrologic and climate change impact analyses in headwater basins of

British Columbia. J Clim 25:5711–5730. https://doi.org/10.1175/JCLI-D-11-00417.1

Bernsteinová J, Bässler C, Zimmermann L et al (2015) Changes in runoff in two neighbouring catchments in the Bohemian Forest related to climate and land cover changes. J Hydrol Hydromechanics 63:342–352. https://doi.org/10.1515/johh-2015-0037

Beudert B, Bässler C, Thorn S et al (2015) Bark beetles increase biodiversity while maintaining drinking water quality. Conserv Lett 8:272–281. https://doi.org/10.1111/CONL.12153

Biggs J, von Fumetti S, Kelly-Quinn M (2016) The importance of small waterbodies for biodiversity and ecosystem services: implications for policy makers. Hydrobiologia 793:3–39. https://doi.org/10.1007/S10750-016-3007-0

Brooks RT (2009) Potential impacts of global climate change on the hydrology and ecology of ephemeral freshwater systems of the forests of the northeastern United States. Clim Change 95:469–483. https://doi.org/10.1007/s10584-008-9531-9

Cannon AJ, Sobie SR, Murdock TQ (2015) Bias correction of GCM precipitation by quantile mapping: how well do methods preserve changes in quantiles and extremes? J Clim 28:6938–6959. https://doi.org/10.1175/JCLI-D-14-00754.1

Cantonati M, Füreder L, Gerecke R et al (2012) Crenic habitats, hotspots for freshwater biodiversity conservation: toward an understanding of their ecology. Freshw Sci 31:463–480. https://doi.org/10.1899/11-111.1

Chan SS, Seidenfaden IK, Jensen KH, Sonnenborg TO (2021) Climate change impacts and uncertainty on spatiotemporal variations of drought indices for an irrigated catchment. J Hydrol. https://doi.org/10.1016/j.jhydrol.2021.126814

Chen JW, Kuo HT, Lin HL (2016) Estimation the hot spring recharge using groundwater numerical model in Jiao-Shi area, Taiwan. In: Proc IEEE Int Conf Adv Mater Sci Eng Innov Sci Eng IEEE-ICAMSE, pp 434–437. https://doi.org/10.1109/ICAMSE.2016.7840315

Choi B, Kang H, Lee WH (2018) Baseflow contribution to streamflow and aquatic habitats using physical habitat simulations. Water 10:1304. https://doi.org/10.3390/W10101304

Cloutier CA, Buffin-Bélanger T, Larocque M (2014) Controls of groundwater floodwave propagation in a gravelly floodplain. J Hydrol 511:423–431. https://doi.org/10.1016/J.JHYDROL.2014.02.014

Conant B (2004) Delineating and quantifying ground water discharge zones using streambed temperatures. Ground Water 42:243–257. https://doi.org/10.1111/J.1745-6584.2004.TB02671.X

Cornelissen T, Diekkrüger B, Bogena H (2013) Using HydroGeoSphere in a forested catchment: how does spatial resolution influence the simulation of spatio-temporal soil moisture variability? Procedia Environ Sci 19:198–207. https://doi.org/10.1016/j.proenv.2013.06.022

Delleur JW (1999) The handbook of groundwater engineering. CRC Press, Boca Raton, FL

De Schepper G, Therrien R, Refsgaard JC et al (2017) Simulating seasonal variations of tile drainage discharge in an agricultural catchment. Water Resour Res 53:3896–3920. https://doi.org/10.1002/2016WR020209

Downing JA, Cole JJ, Duarte CM et al (2012) Global abundance and size distribution of streams and rivers. Inl Waters 2:229–236. https://doi.org/10.5268/IW-2.4.502

Dwire KA, Mellmann-Brown S, Gurrieri JT (2018) Potential effects of climate change on riparian areas, wetlands, and groundwater-dependent ecosystems in the Blue Mountains, Oregon, USA. Clim Serv 10:44–52. https://doi.org/10.1016/J.CLISER.2017.10.002

Estrela-Segrelles C, Gómez-Martínez G, Pérez-Martín MÁ (2023) Climate change risks on Mediterranean river ecosystems and adaptation measures (Spain). Water Resour Manag. https://doi.org/10.1007/S11269-023-03469-1/FIGURES/6

Fleckenstein JH, Niswonger RG, Fogg GE (2006) River-aquifer interactions, geologic heterogeneity, and low-flow management. Ground Water 44:837–852. https://doi.org/10.1111/j.1745-6584.2006.00190.x

Frei S, Fleckenstein JH, Kollet SJ, Maxwell RM (2009) Patterns and dynamics of river-aquifer exchange with variably-saturated flow using a fully-coupled model. J Hydrol 375:383–393. https://doi.org/10.1016/j.jhydrol.2009.06.038

Frei S, Lischeid G, Fleckenstein JH (2010) Effects of micro-topography on surface–subsurface exchange and runoff generation in a virtual riparian wetland—a modeling study. Adv Water Resour 33:1388–1401. https://doi.org/10.1016/J.ADVWATRES.2010.07.006

Glaser B, Klaus J, Frei S et al (2016) On the value of surface saturated area dynamics mapped with thermal infrared imagery for modeling the hillslope-riparian-stream continuum. Water Resour Res 52:8317–8342. https://doi.org/10.1002/2015WR018414

Goderniaux P, Brouyère S, Fowler HJ et al (2009) Large scale surface-subsurface hydrological model to assess climate change impacts on groundwater reserves. J Hydrol 373:122–138. https://doi.org/10.1016/j.jhydrol.2009.04.017

Goderniaux P, Brouyère S, Wildemeersch S et al (2015) Uncertainty of climate change impact on groundwater reserves - application to a chalk aquifer. J Hydrol. https://doi.org/10.1016/j.jhydrol.2015.06.018

Gosling SN, Zaherpour J, Mount NJ et al (2017) A comparison of changes in river runoff from multiple global and catchment-scale hydrological models under global warming scenarios of 1 °C, 2 °C and 3 °C. Clim Chang 141:577–595. https://doi.org/10.1007/S10584-016-1773-3

Huang S, Krysanova V, Österle H, Hattermann FF (2010) Simulation of spatiotemporal dynamics of water fluxes in Germany under climate change. Hydrol Process 24:3289–3306. https://doi.org/10.1002/hyp.7753

Huntington JL, Niswonger RG (2012) Role of surface-water and groundwater interactions on projected summertime streamflow in snow dominated regions: an integrated modeling approach. Water Resour Res. https://doi.org/10.1029/2012WR012319

HydroAlgorithmics Pty Ltd (2016) AlgoMesh User Guide. 257

IPCC (2014) Climate Change 2014: synthesis report. Contribution of Working Groups I, II and III to the Fifth Assessment Report of the Intergovernmental Panel on Climate Change [Core Writing Team, R.K. Pachauri and L.A. Meyer (eds.)]. IPCC, Geneva, Switzerland

Karvonen A, Rintamäki P, Jokela J, Valtonen ET (2010) Increasing water temperature and disease risks in aquatic systems: climate change increases the risk of some, but not all, diseases. Int J Parasitol 40:1483–1488. https://doi.org/10.1016/J.IJPARA.2010.04.015

Kaule L, Frei S (2022) Analysis of drought conditions and their impacts in a headwater stream in the Central European lower mountain ranges. Reg Environ Chang. https://doi.org/10.1007/s10113-022-01926-y

Kaule R, Gilfedder BS (2021) Groundwater dominates water fluxes in a headwater catchment during drought. Front Water 3:89. https://doi.org/10.3389/FRWA.2021.706932/BIBTEX

Kim MK, Kim S, Kim J et al (2016) Statistical downscaling for daily precipitation in Korea using combined PRISM, RCM, and quantile mapping: part 1, methodology and evaluation in historical simulation. Asia-Pac J Atmos Sci 52:79–89. https://doi.org/10.1007/S13143-016-0010-3

Krause S, Bronstert A, Zehe E (2007) Groundwater-surface water interactions in a North German lowland floodplain - Implications for the river discharge dynamics and riparian water balance. J Hydrol 347:404–417. https://doi.org/10.1016/j.jhydrol.2007.09.028

Kristensen KJ, Jensen SE (1975) A model for estimating actual evapotranspiration from potential evapotranspiration. Hydrol Res 6:170–188. https://doi.org/10.2166/nh.1975.0012

López-de Sancha A, Roig R, Jiménez I et al (2022) Impacts of damming and climate change on the ecosystem structure of headwater streams: a case study from the Pyrenees. Inl WATERS 12:434–450. https://doi.org/10.1080/20442041.2021.2021776

Majdi N, Colls M, Weiss L et al (2020) Duration and frequency of non-flow periods affect the abundance and diversity of stream meiofauna. Freshw Biol 65:1906–1922. https://doi.org/10.1111/FWB.13587

Majerova M, Neilson BT, Schmadel NM et al (2015) Impacts of beaver dams on hydrologic and temperature regimes in a mountain stream. Hydrol Earth Syst Sci 19:3541–3556. https://doi.org/10.5194/HESS-19-3541-2015

Maraun D (2013) Bias correction, quantile mapping, and downscaling: revisiting the inflation issue. J Clim 26:2137–2143. https://doi.org/10.1175/JCLI-D-12-00821.1

Marke T (2008) Development and application of a model interface to couple land surface models with regional climate models for climate change risk assessment. Ludwig Maximilian University of Munich

Marx A, Kumar R, Thober S et al (2018) Climate change alters low flows in Europe under global warming of 1.5, 2, and 3 °C. Hydrol Earth Syst Sci 22:1017–1032. https://doi.org/10.5194/HESS-22-1017-2018

Miller MP, Buto SG, Susong DD, Rumsey CA (2016) The importance of base flow in sustaining surface water flow in the upper Colorado River Basin. Water Resour Res 52:3547–3562. https://doi.org/10.1002/2015WR017963

Min L, Shen Y, Pei H (2015) Estimating groundwater recharge using deep vadose zone data under typical irrigated cropland in the piedmont region of the North China Plain. J Hydrol 527:305–315. https://doi.org/10.1016/J.JHYDROL.2015.04.064

Misra D, Daanen RP, Thompson AM (2011) Base flow/groundwater flow. In: Singh VP, Singh P, Haritashya UK (eds) Encyclopedia of earth sciences series. Springer, Dordrecht. https://doi.org/10.1007/978-90-481-2642-2_36

Molano-Leno L, Kohfahl C, Martínez Suárez DJ et al (2018) Investigating the impact of climate change on groundwater recharge using a high precision meteo lysimeter in a dune belt of the Doñana National Park. In: Calvache M, Duque C, Pulido-Velazquez D (eds) Groundwater and global change in the western Mediterranean area. Environmental earth sciences. Springer, Cham

Moriasi DN, Arnold JG, Van LMW et al (2007) Model evaluation guidelines for systematic quantification of accuracy in watershed simulations. Trans ASABE 50:885–900. https://doi.org/10.13031/2013.23153

Natkhin M, Steidl J, Dietrich O et al (2012) Differentiating between climate effects and forest growth dynamics effects on decreasing groundwater recharge in a lowland region in Northeast Germany. J Hydrol 448–449:245–254. https://doi.org/10.1016/j.jhydrol.2012.05.005

Ngai ST, Tangang F, Juneng L (2017) Bias correction of global and regional simulated daily precipitation and surface mean temperature over Southeast Asia using quantile mapping method. Glob Planet Chang 149:79–90. https://doi.org/10.1016/J.GLOPLACHA.2016.12.009

Niswonger RG, Fogg GE (2008) Influence of perched groundwater on base flow. Water Resour Res 44:3405. https://doi.org/10.1029/2007WR006160

Nyquist JE, Freyer PA, Toran L (2008) Stream bottom resistivity tomography to map ground water discharge. Ground Water 46:561–569. https://doi.org/10.1111/j.1745-6584.2008.00432.x

O'Connor BL, Harvey JW (2008) Scaling hyporheic exchange and its influence on biogeochemical reactions in aquatic ecosystems.

Water Resour Res 44:1–17. https://doi.org/10.1029/2008WR007160

Partington D, Brunner P, Frei S et al (2013) Interpreting streamflow generation mechanisms from integrated surface-subsurface flow models of a riparian wetland and catchment. Water Resour Res 49:5501–5519. https://doi.org/10.1002/wrcr.20405

Peralta-Tapia A, Sponseller RA, Ågren A et al (2015) Scale-dependent groundwater contributions influence patterns of winter baseflow stream chemistry in boreal catchments. J Geophys Res Biogeosciences 120:847–858. https://doi.org/10.1002/2014JG002878

Power G, Brown RS, Imhof JG (1999) Groundwater and fish—insights from northern North America. Hydrol Process 13:401–422. https://doi.org/10.1002/(SICI)1099-1085(19990228)13:3

Rajczak J, Kotlarski S, Schär C (2016) Does quantile mapping of simulated precipitation correct for biases in transition probabilities and spell lengths? J Clim 29:1605–1615. https://doi.org/10.1175/JCLI-D-15-0162.1

Reiter P, Gutjahr O, Schefczyk L et al (2018) Does applying quantile mapping to subsamples improve the bias correction of daily precipitation? Int J Climatol 38:1623–1633. https://doi.org/10.1002/JOC.5283

Richter BD, Baumgartner JV, Wigington R, Braun DP (1997) How much water does a river need? Freshw Biol 37:231–249. https://doi.org/10.1046/j.1365-2427.1997.00153.x

Ringard J, Seyler F, Linguet L (2017) A quantile mapping bias correction method based on hydroclimatic classification of the Guiana shield. Sensors 17:1413. https://doi.org/10.3390/S17061413

Seibert J (1997) Estimation of parameter uncertainty in the HBV ModelPaper presented at the Nordic hydrological conference (Akureyri, Iceland - August 1996). Hydrol Res 28:247–262. https://doi.org/10.2166/NH.1998.15

Taie Semiromi M, Koch M (2020) How do gaining and losing streams react to the combined effects of climate change and pumping in the Gharehsoo River Basin, Iran? Water Resour Res. https://doi.org/10.1029/2019WR025388

Therrien R, McLaren R, Sudicky E, Panday S (2008) HydroGeoSphere a threedimensional numerical model describing fully-integrated subsurface and surface flow and solute transport (manual). University of Waterloo: Groundwater Simulations Group

Van Vliet MTH, Franssen WHP, Yearsley JR et al (2013) Global river discharge and water temperature under climate change. Glob Environ Chang 23:450–464. https://doi.org/10.1016/J.GLOENVCHA.2012.11.002

Ward AS, Wondzell SM, Schmadel NM, Herzog SP (2020) Climate change causes river network contraction and disconnection in the H.J. Andrews experimental forest, Oregon, USA. Front Water 2:1–10. https://doi.org/10.3389/frwa.2020.00007

Weigel AP, Knutti R, Liniger MA, Appenzeller C (2010) Risks of model weighting in multimodel climate projections. J Clim 23:4175–4191. https://doi.org/10.1175/2010JCLI3594.1

Whitehead PG, Wilby RL, Battarbee RW et al (2009) A review of the potential impacts of climate change on surface water quality. Hydrol Sci J 54:101–123. https://doi.org/10.1623/HYSJ.54.1.101

Wunsch A, Liesch T, Broda S (2022) Deep learning shows declining groundwater levels in Germany until 2100 due to climate change. Nat Commun 131(13):1–13. https://doi.org/10.1038/s41467-022-28770-2